

# Intensified, Kilogram-Scaled, and Environment-Friendly: Chemoenzymatic Synthesis of Bio-Based Acylated Hydroxystyrenes

Philipp Petermeier, Pablo Domínguez de María, Emil Byström, and Selin Kara\*

Cite This: *ACS Sustainable Chem. Eng.* 2024, 12, 12869–12878

Read Online

ACCESS |



Metrics &amp; More



Article Recommendations



Supporting Information

**ABSTRACT:** Lignin-derived styrene derivatives are versatile building blocks for the manufacture of biobased polymers. As shown previously, phenol-protected hydroxystyrenes are accessible under industrially sound conditions ( $>100 \text{ g L}^{-1}$ ,  $>95\%$  yield) by subjecting biogenic phenolic acids to enzymatic decarboxylation and base-catalyzed acylation in nonaqueous media (wet cyclopentyl methyl ether, CPME). Herein, we demonstrate the production of 1 kg of 4-acetoxy-3-methoxystyrene in a 10 L reactor and present practical adjustments to the up- and downstream processing that warrant a straightforward process and high isolated yields. Additionally, an environmental assessment is conducted, starting with a thorough *E* factor analysis to identify the sources that contribute most to the environmental burden (solvent and downstream processing). Also, the total  $\text{CO}_2$  production of the process is studied, including contributions from energy use and the treatment of generated wastes. The energy impact is evaluated through thermodynamic analysis, and the environmental footprint contributions by wastes—organic and aqueous fractions—are assessed based on  $\text{CO}_2$  emissions from solvent incineration and wastewater treatment, respectively. Overall, the holistic assessment of the process, its optimization, scale-up, product isolation, and environmental analysis indicate the feasibility of multistep chemoenzymatic reactions to deliver high-volume, low-value chemicals from biorefineries.

**KEYWORDS:** reaction cascade, styrene alternatives, carbon dioxide equivalents, green solvents, phenolic acids, polymer precursors



## INTRODUCTION

The nonenergy use of fossil raw materials (oil, gas, coal) in the 20 largest countries by GDP amounts to  $\sim 8.3\%$  of their total annual supply. At the same time, their energy use by the manufacturing sector is  $\sim 23.7\%$ , with transportation, households, agriculture, and commerce accounting for the rest.<sup>1</sup> Thus, if the chemical industry is to contribute to a global circular economy, it is necessary to transition to the efficient use of more biobased or recycled raw materials. Particularly high-volume market segments take in substantial resources to produce major products, e.g., plastics, synthetic fibers, synthetic rubber, dyes, or fertilizers. With the worldwide production of plastics exceeding 400 Mt in 2022 and projected continued growth in the coming decades,<sup>2</sup> the need for responsible production and consumption of plastics must be highlighted.

Against this background, we were inspired by recent advances in the polymerization of biobased styrene derivatives that make them key precursors to furnish emerging synthetic polymers.<sup>3–11</sup> Their appeal as precursors is 2-fold: on the one hand, they can be derived from lignocellulosic biomass, what confers them untapped opportunities for future biomaterial uses with high sustainability profiles at scale<sup>12–14</sup>; on the other hand, their phenolic structure provides scope for simple and—if necessary—reversible modifications to tune application-specific material properties.<sup>7,10</sup> In fact, access to platform chemicals, which can simultaneously be easily tailored for different applications, is a crucial precondition for creating diverse commercialization paths for various products. The potential of

phenolic styrenes in this regard is evidenced by reports of multifaceted applications such as in polymer blends,<sup>3</sup> resins,<sup>4</sup> copolymers,<sup>5–7</sup> well-defined polymers of controlled tacticities,<sup>9</sup> polymer linkers and diluents,<sup>10</sup> self-healing materials,<sup>15</sup> or adhesives and hydrogels.<sup>16,17</sup> Considering that the annual highly energy-intensive production of styrene from crude oil is in the range of 15 Mt with a market value exceeding \$43 billion, pivoting to innovative biogenic alternatives may have a drastic impact.<sup>18,19</sup>

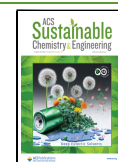
With these promising aspects, we set out to establish productive, mild, and scalable synthetic routes that may give access to these monomers starting from lignin-derived phenolic acids.<sup>20,21</sup> First, we introduced a chemoenzymatic one-pot two-step cascade that proceeds entirely in the (potentially) renewable solvent cyclopentyl methyl ether (CPME)<sup>22</sup> and eliminates the need for intermediary workup steps, the stoichiometric use of hazardous reagents, and nonrecommended solvents.<sup>20</sup> For the initial decarboxylation step, we harnessed phenolic acid decarboxylase from *Bacillus subtilis* (BsPAD, PDB entry: 2P8G)<sup>23</sup> immobilized on a macroporous methacrylate carrier (ECR8415F), rendering the heteroge-

Received: May 2, 2024

Revised: August 1, 2024

Accepted: August 1, 2024

Published: August 15, 2024



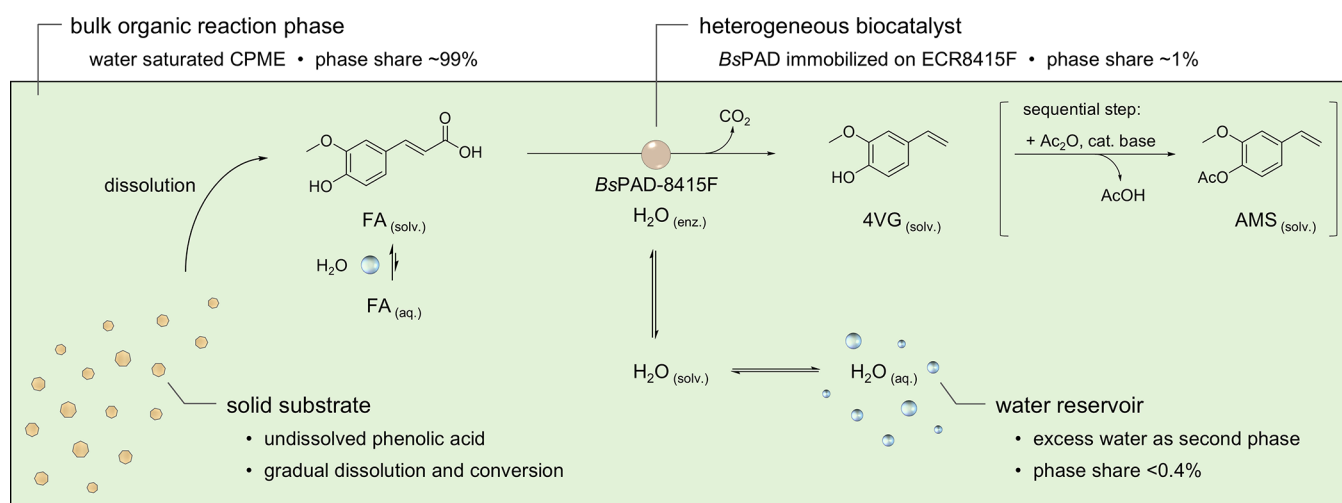


**Figure 1.** Chemoenzymatic reaction system with its underlying equilibria, constituent phases, and process steps. The reaction cascade accepts phenolic acid substrates such as *p*-coumaric acid, caffeic acid, or ferulic acid and is illustrated with the latter. The proportions of different phases (phase shares) are given on a mass fraction basis and do not consider the solid substrate phase, as it is not present at low concentrations and both gradually and fully consumed at high concentrations.<sup>20,21</sup> Abbreviations: CPME, cyclopentyl methyl ether; FA, ferulic acid; 4VG, 4-vinylguaiaicol; AMS, 4-acetoxy-3-methoxystyrene; AcOH, acetic acid; BsPAD, phenolic acid decarboxylase from *Bacillus subtilis*; solv., partitioning in organic solvent phase; aq., partitioning in aqueous phase; enz., partitioning in enzyme pseudophase.

neous biocatalyst BsPAD-8415F. This was combined, in a subsequent step, with inorganic base catalysis for the protection of the phenol group *via* acetylation. The overarching strategy proved effective, robust, and free of significant byproduct formation, yet the product titers ( $19 \text{ g L}^{-1}$ ,  $0.1 \text{ M}$ ) remained below industrially relevant levels, where more than  $100 \text{ g L}^{-1}$  are typically required.<sup>24</sup>

Consequently, emphasis was put on process intensification, revealing the intricacies that limited the biocatalytic transformation.<sup>21,25</sup> As illustrated in Figure 1, the substrate (*e.g.*, ferulic acid, FA) gradually dissolves and partitions between the two liquid phases, the predominant organic phase that makes up more than 99% of all liquid and the small aqueous second phase (as the reaction is performed in slightly oversaturated wet CPME). Based on the disparate liquid volumes and the significantly greater substrate solubilities in CPME than in water (for FA:  $31$  vs  $0.92 \text{ g L}^{-1}$ ), it can be estimated that  $>99.9\%$  of all dissolved substrate will accumulate in the organic phase. From there it is transferred to the immobilized enzyme (BsPAD-8415F) and converted to the respective hydroxystyrene (*e.g.*, 4-vinylguaiaicol, 4VG) of even higher solubility in the organic media.<sup>20</sup> Importantly, the enzymatic activity requires a minimum water activity  $a_w$  and is optimal at  $a_w = 1$ , which is practically fulfilled by using water saturated solvent and moist enzyme beads. However, as the reaction progresses, the proportion of polar species (*e.g.*, FA, 4VG) in the bulk organic phase increases, which enhances its water uptake capacity. This is unfavorable, as the immobilized enzyme and the organic phase compete for dissolved water and are in equilibrium with their respective water activities. Hence, concentration of the reaction system without adequate countermeasures would eventually suppress enzymatic activity. Fortunately, incorporating water reservoirs of minimal yet sufficient size can effectively balance the increased need for dissolved water without causing negative interference with the overall reaction system (*e.g.*, negligible effects on substrate dissolution). With this, the sequential cascade was intensified to industrially sound product titers of about  $400 \text{ g L}^{-1}$ .<sup>21</sup>

The reported chemoenzymatic system may become quite useful when it comes to industrial applications. Crucially, the combination of biocatalysis with chemical steps can be achieved by compatible media and conditions, *i.e.*, the use of wet CPME for the entire process. Besides, the approach may represent an excellent example of how bulk chemicals can be produced biocatalytically, especially when intensified systems are established and process conditions are understood and well controlled.

Following these considerations, some aspects remain to be addressed: First, the scalability of the reaction, including analysis of potential bottlenecks in up- or downstream processing. Second, the provision of a careful environmental assessment of the optimized and scaled-up synthetic system, to substantiate its greenness with solid metrics. In this study, we provide a process scale-up to a  $10 \text{ L}$  reactor and scrutinize the environmental footprint of the optimized reaction in terms of the *E* factor<sup>26,27</sup> [ $\text{kg}_{\text{waste}} \text{ kg}_{\text{product}}^{-1}$ ] and the total carbon dioxide release (TCR).<sup>28–31</sup>

## RESULTS AND DISCUSSION

### Exploratory Laboratory Scale: Refining the Workup.

Prior to the on-scale deployment of the intensified process, we aimed for preparative experiments in  $200 \text{ mL}$  benchtop lab reactors at concentrations of  $500 \text{ mM}$ . However, this required adaptations to the workup, as crude product solutions from intensified syntheses on microcentrifuge scales turned gelatinous upon cooling, hampering the downstream processing. According to our established routine,<sup>20</sup> the enzymatic decarboxylation at  $30 \text{ }^\circ\text{C}$  was followed by the recovery of biocatalyst and addition of base catalyst for acylation using carboxylic anhydrides at  $80\text{--}90 \text{ }^\circ\text{C}$  (see Figure 2). The formation of gelatinous phases after reaction cooling was observed for product titers of  $>0.1 \text{ M}$ , presumably caused by the rapid precipitation of the acylated hydroxystyrene. Attempts to control and exploit the precipitation for physical product recovery by filtration turned out unsuccessful. We hypothesized that the high concentrations of polar carboxylic acid byproduct (acetic acid) adversely affect the solubility of

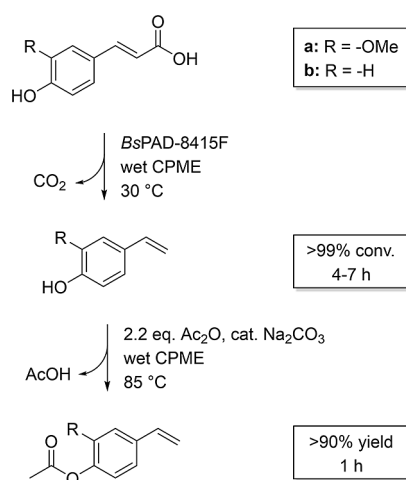


**Figure 2.** Preparatory syntheses performed at 120 mL lab scale using (a) ferulic acid and (b) *p*-coumaric acid as starting materials at concentrations of 500 mM (82–97 g L<sup>-1</sup>). The reaction conditions were similar to the ones applied at 1 mL, only with a slight reduction in reaction temperature from 90 to 85 °C during acylation, due to technical limitations by the water heater thermostat employed. Details of the procedures are given in the [Supporting Information](#).

the less polar acylated hydroxystyrenes. Thus, selective removal of these acid species should significantly increase product solubility and prevent unintended precipitation. To achieve this, a hot quench with aqueous Na<sub>2</sub>CO<sub>3</sub> was adopted, in which the reaction mixture was tempered to 60 °C after the two-step reaction sequence, leading to a stable homogeneous mixture. By using equimolar amounts of carbonate, all carboxylic acid (and residual anhydride) were effectively

converted into sodium carboxylate and extracted into the aqueous phase. The two phases (product/CPME and sodium acetate/H<sub>2</sub>O) were easily separated, and the organic phase was ready for product isolation by drying and solvent removal.

Once the refined workup was established, the reaction cascade was conducted on a 120 mL lab scale using the SpinChem rotating bed reactor S2 in a 200 mL baffled glass reactor (see [Supporting Information](#)). In this setup, the biocatalyst beads are compartmentalized in a cage-like cylindrical structure that simultaneously acts as the agitator, enabling effective biocatalyst deployment and removal in the reaction sequence.<sup>32</sup> For comparison, the two substrates ferulic acid and *p*-coumaric acid (*p*CA) were both used at 500 mM loading, and acetic anhydride was employed as the acylation agent (see [Figure 2](#)). Gratifyingly, the processes yielded the corresponding acylated hydroxystyrenes 4-acetoxy-3-methoxystyrene (AMS) and 4-acetoxystyrene (AS) in high yields of 10.8 g (93%) and 9.3 g (95%), respectively, confirming that the developed synthetic route can be scaled once the hurdles observed in the workup were resolved.

**Technical Synthesis at 10 L Scale.** Once the refined workup procedure was demonstrated on the lab scale, the reaction cascade was conducted on a 10 L scale to produce 1 kg AMS in a single batch. An important aspect en route to scale-up is the safe handling of chemicals and devices in the lab. For this, we customized the SpinChem rotating bed reactor Complete S4, enabling safe and time-efficient operation with the reaction system at hand. Importantly, to prevent the formation of an explosive atmosphere, we ensured that the agitator was operated with a remote-controlled compressed air-driven motor, all metallic parts of the reactor and reactor frame were grounded, the complete reactor was housed in a ventilated cabinet, and the electrical thermostat for the control

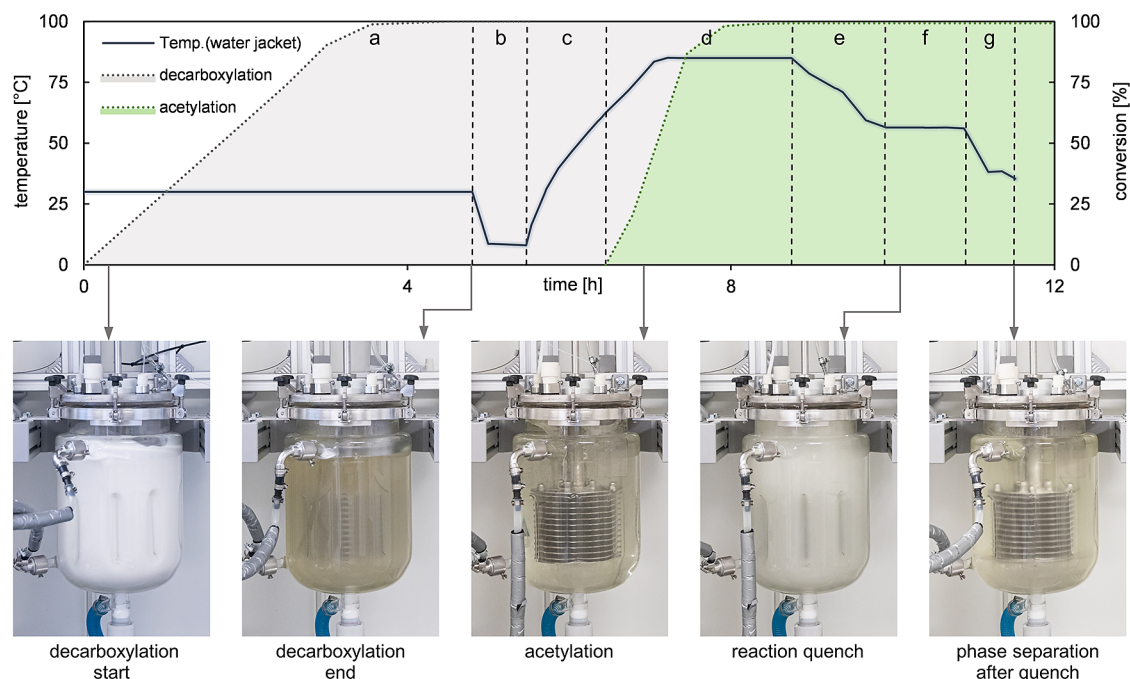


**Figure 3.** Chemoenzymatic production of 4-acetoxy-3-methoxystyrene (AMS) in a 10 L baffled glass vessel using the Complete S4 model of the rotating bed reactor. The temperature profile (blue line), reaction progress (gray: decarboxylation; green: acetylation), and images of the reactor are given for the various stages of the synthetic process: (a) biocatalytic decarboxylation, (b) exchange of the biocatalyst for the inorganic base catalyst, (c) warm-up phase prior addition of acetic anhydride, (d) chemocatalytic acetylation, (e) gradual cool-down phase prior quenching, (f) reaction quench using aqueous sodium carbonate, and (g) cooling of the reactor prior drainage.



of the water jacket temperature was placed outside of the ventilated cabinet. An annotated picture of the reactor with its essential safety-relevant components is provided in the [Supporting Information](#).

When defining the operating procedure, we considered that individual reactor charging steps may become more cumbersome and time-consuming at scale, which makes a proper sequence of steps more crucial to avoid undesired events such as early reaction starts, runaway reactions, or catalyst deactivation. For the biocatalytic decarboxylation, previous studies have shown that the biocatalyst BsPAD-8415F is sensitive to a lack of enzyme hydration.<sup>20,21</sup> Since a temporary and/or local lack of water in the immediate surrounding of the biocatalyst may occur during reactor charging, we experimentally assessed the severity of the worst-case scenario: BsPAD-8415F beads were air-dried and then suspended in a dry solution of FA in CPME for 10 and 120 min, respectively, before the water required for water saturation was added and the reaction progress tracked. As a comparison to the immobilized enzyme, lyophilized cell-free extract was subjected to the same conditions. This revealed that the belated introduction of water to the dry reaction system recovers enzyme activity in all cases, albeit to a weaker extent in the case of prolonged exposure to dry conditions. Moreover, the relative loss in enzyme activity was similar in either biocatalyst preparation (Supplementary [Figure S1](#)). From this, we concluded that maintaining wet conditions for the biocatalyst during reactor charging is advantageous but not critical as the immobilized enzyme displays sufficient resilience to transient dry conditions and can therefore be deployed in scaled reactor systems.

For the second reaction step, the chemocatalytic acylation, the acyl donor was added stepwise, thus implementing a reagent-limited reaction control strategy to avoid exothermic runaway scenarios. Considering the target of 1 kg isolated AMS and the nominal, minimum, and maximum operation volumes of the SpinChem Complete S4 reactor system, the required process intensity was determined to be 630 mM (120 g L<sup>-1</sup>). Although we have previously demonstrated on a 1 mL scale that this reaction cascade is highly productive also at concentrations of up to 400 g L<sup>-1</sup>,<sup>21</sup> we established—for this first-ever implementation on 10 L scale—reaction intensities that were close to our preliminary preparative syntheses at 500 mM (96 g L<sup>-1</sup>). In addition to the above-mentioned measure on reaction control and the well-dimensioned reactor cooling system, this decision was also taken to increase operational safety by preempting unforeseen events that might arise from simultaneous excessive up-scaling of process capacity and intensity.

The actual implementation of the reaction cascade on this scale proved eminently straightforward. For the detailed operational procedure and safety measures involved see the [Supporting Information](#). The main difference to previous scales was the—depending on the process stage—much murkier or more intensely colored reaction mixture, a direct consequence of the scale-associated increase in layer thickness. As shown in [Figure 3](#), the reaction system started as a suspension of ferulic acid in wet CPME and turned into a murky solution of 4-vinylguaiacol in CPME by the end of the first reaction (decarboxylation). At this stage, the reaction mixture was cooled to lower the vapor pressure of all components involved (flammable solvent, odorous intermediate) before the reactor was opened, the biocatalyst recovered, the inorganic base

catalyst added, the reactor system closed, and heated for subsequent acylation. Following close-to-complete conversion (~99%) in the second reaction step, the reaction mixture was cooled to the quenching temperature, mixed with water, and treated with equimolar amounts of sodium carbonate. The vigorous release of CO<sub>2</sub> during this workup step was well-controlled by the gradual addition of the quenching agent. Eventually, our setup and routine gave access to a concentrated solution of AMS in CPME of immediate good purity in a single working day. Solvent removal by (nonoptimized) distillation recovered 84% of all CPME used and at the same time yielded 1060 g AMS (97%) as faintly greenish oil in high purity (HPLC: 99.4%, <sup>1</sup>H NMR: 98%).

**Process Optimization Outlook.** The overall synthetic approach has proven to be scalable regarding both upstream and downstream processing. Looking beyond the current stage, and to avoid the cumbersome intermediary step of reactor refitting and biocatalyst recovery, an alternative semicontinuous two-reactor configuration can be envisaged. In such a setup, the first reactor (R1) would enable the biocatalytic decarboxylation, while the acylation would be conducted in a second downstream reactor (R2). For this, the entire reaction mixture would be transferred from R1 to R2 between the two consecutive reaction steps. This configuration would come with several advantages, such as greater automation capability, intrinsically higher operational safety (the system always remains closed), less downtime for cleaning, and the possibility of semicontinuous operation allowing for immediate reuse of the biocatalyst in another batch without delay, hence making the most out of it.

**Analysis of Performance Metrics.** At this point, the syntheses carried out during process optimization and scale-up are compared by scale, product, and key performance indicators ([Table 1](#)). Process intensification was demonstrated

**Table 1. Details and Key Metrics of Preparative Acyl-Protected Hydroxystyrenes Syntheses**

entry	1 <sup>a</sup>	2	3	4
product	AMS	AMS	AS	AMS
reaction volume [L]	1.0	0.12	0.12	10
product titer [mM]	100	500	500	630
yield [g]	18.3	10.8	9.3	1,060
yield [%]	96	93	95	97
<sup>1</sup> H NMR purity [%]	95	99	99	98
HPLC purity <sup>b</sup> [%]	99	98.4	99.9	99.4
volumetric productivity <sup>c</sup> [g L <sup>-1</sup> h <sup>-1</sup> ]	1.6	17	8.5	12
biocatalytic productivity [mmol g <sub>cat</sub> <sup>-1</sup> h <sup>-1</sup> ]	6.4	17.9	6.0	17.5
data from	ref 20	this study	this study	this study

<sup>a</sup>Data from a previous experiment by the authors from an early process development stage, incorporated to provide a meaningful point of reference.<sup>20</sup> <sup>b</sup>At a detector wavelength of 254 nm. <sup>c</sup>Over two reaction steps, excluding workup.

on a preparative scale from 100 to 630 mM and—given the adjusted hot quench routine—consistently produced high crude product yields and purities. For all cases, volumetric productivities were calculated from the isolated yield [g], the reaction volume [L], and the operation time [h] over the two reaction steps excluding the workup. This revealed a substantial improvement of productivity by roughly 10-fold

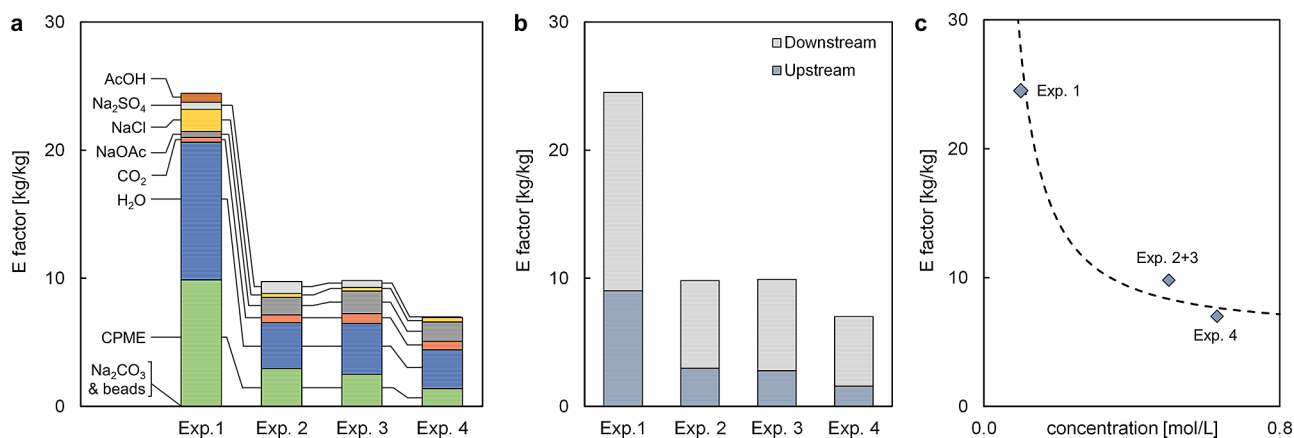


**Figure 4.** Reduction of  $E$  factor due to process intensification and optimized (re)use of chemicals and solvent. (a) Provides a breakdown by type of waste with “beads” referring to the waste fraction of consumed solid biocatalyst beads BsPAD-8415F. (b) Classifies waste stream contributions based on their origin during synthesis (upstream) or workup and product isolation (downstream). (c) Illustrates the  $E$  factor reduction during process optimization, intensification, and upscaling, with the dashed line approximating the effect of process intensification alone. The different experiments refer to the following syntheses: Exp. 1: AMS (0.1 M at 1.0 L); Exp. 2: AMS (0.5 M at 0.12 L); Exp. 3: AS (0.5 M at 0.12 L); and Exp. 4: AMS (0.63 M at 10 L).

as the laboratory scale cascade was intensified from 100 to 500 mM AMS (cf. entry 1 and 2). However, with further scaling to the 10 L system (cf. entry 4), we experienced a drop in the volumetric productivity from 17 to 12 g L<sup>-1</sup> h<sup>-1</sup>. This is explained by (i) the intermediary disassembly of the agitator for catalyst exchange, which was more time-consuming at the 10 L scale, and (ii) the slower heating of the reactor due to a lack of thermal heating output (1200 W) by the thermostat used. Based on this, it is expected that a more adequate thermostat, additional insulation, and the previously proposed semicontinuous two-reactor setup will enable technical-scale volumetric productivities that are at least on par with lab scale. Moreover, we have shown in previous work<sup>21</sup> that the chemoenzymatic conversion can be pushed to titers of at least 2 M (~400 g L<sup>-1</sup>). Hence, contingent on safe technical implementation and preserved effectiveness of the hot quench strategy at these concentrations, this synthetic approach has still much potential to be explored.

Concerning the performance of the biocatalytic decarboxylation step on its own, we calculated the biocatalytic productivity in [mmol] of substrate converted per gram of catalyst and operation time. Here, we find virtually identical results for both intensified AMS syntheses in either 0.12 and 10 L scale (cf. entry 2 and 4). This indicates that all factors essential for the intensified biotransformation were identified and well-controlled during upscaling. Arguably the most important factor is the precisely adjusted amount of reservoir water that is required to maintain enzymatic activity throughout. As this was not as well controlled in the first experiment (cf. entry 1), the respective biocatalytic productivity was inferior there. Furthermore, the likewise lower productivity for the conversion of *p*CA (cf. entry 3) is attributed to the generally lower affinity of BsPAD toward this substrate.

**Environmental Footprint:  $E$  Factor and Total CO<sub>2</sub> Release.** Having optimized and scaled the synthesis of biobased acetylated hydroxystyrene monomers in a straightforward sequential two-step cascade, its environmental impact was assessed too. The key features of this synthetic approach concerning its suspected greenness would be its intensified nature, the reusable biocatalyst, and the easily recoverable

(potentially biogenic) organic solvent.<sup>20,21</sup> For the quantitative analysis of material and waste streams, gate-to-gate system boundaries that include both reaction steps—decarboxylation and acetylation —, the workup, and the product isolation to afford one kilogram product were considered (all steps are illustrated in Supplementary Figure S7).<sup>33</sup> Other steps in the overall value chain from lignocellulosic biomass to the final synthetic polymer, such as raw material extraction, processing, transportation, and monomer polymerization were not included, since the aim was to evaluate the optimized chemoenzymatic step. Future more holistic assessments should include these cradle-to-gate strategies further, to define the overall picture of the synthetic route.

In the first step, the  $E$  factor ( $\text{kg}_{\text{waste}} \text{kg}_{\text{product}}^{-1}$ )<sup>26</sup> was determined for preparative syntheses with different substrate loadings and reaction volumes. The overall waste streams were broken down into their respective compositions, and the contributions of both the upstream and the downstream were assessed (Figure 4a,b). For an overview of the material flows be referred to Supplementary Figure S7. Finally, an extrapolation on the  $E$  factor dependence of the process intensity was made (Figure 4c). Starting from the earlier synthesis of 0.1 M AMS on the 1 L scale in Figure 4a (Exp. 1),<sup>20</sup> it became clear that water and CPME are by far the largest contributors to the total waste generated, consistent with common literature observations.<sup>33,34</sup> To improve the environmental burden, a combination of process intensification and a more circumspect use of water in the reaction quench proved to be highly effective and cut the specific waste generation from ~25 to ~10 kg kg<sup>-1</sup>. This was observed in both 0.5 M syntheses of AMS and AS, which were conducted as preliminary experiments before upscaling to the 10 L system (cf. Exp. 2 and 3).

Further process intensification and savings in desiccant (Na<sub>2</sub>SO<sub>4</sub>) consumption due to cleaner phase separation further lowered the  $E$  factor to 7.0 kg kg<sup>-1</sup> for the synthesis of AMS on the 10 L scale (Exp. 4). The effects of the measures taken can be seen in the drastically lowered fractions of CPME, water, and Na<sub>2</sub>SO<sub>4</sub> in Figure 4a. These calculations included all water used in direct contact with the reaction medium (water saturated reaction system, quenching, washing), as it accrues in

contaminated form and eventually needs to be subjected to wastewater treatment (see below). In contrast, water used as a heating medium in the reactor's tempered water jacket was not considered a waste stream as it remains uncontaminated and ideally is completely recirculated in the closed thermostat loop. Concerning the solvent CPME, all that could not be recovered by distillation during product isolation was considered waste. In our processing setup, including our batch-wise operated benchtop distillation apparatus, ~80% of the total CPME was recovered and reusable. Although the biocatalyst beads BsPAD-8415F only make up a minuscule fraction of the overall waste profile (<0.1 kg kg<sup>-1</sup>), they are 100% recoverable due to the deployment in the rotating bed reactor agitator and retain around 71% catalytic activity after initial use. This allows the beads to be reused at least 2–3 times, further reducing their waste contribution. For more calculation details, see Supplementary Tables S1–4; for material reusability, see Supplementary Figures S9 and S10.

We also evaluated the waste contribution from upstream enzyme expression, harvesting, and immobilization (Supplementary Figure S8) and found that a total of 76.7 kg waste was generated per 1 kg BsPAD-8415F beads. Considering that the production of 1.06 kg AMS required 90 g of these beads and that these lost 29% catalytic activity, the aliquot additional *E* factor contribution to the overall process by the current biocatalyst production is 1.9 kg kg<sup>-1</sup>. This highlights the potency vested in highly productive catalysts and simultaneously points toward the positive effects of further improved catalyst recycling.

Another important aspect observed is that the largest fraction of waste originates from the downstream processing (Figure 4b). While contributions from both up- and downstream processes were effectively lowered with each iteration, downstream steps proved consistently more wasteful. All this despite the use of a straightforward reaction system with a minimum number of bulk phase constituents simplifying product isolation, the use of a single solvent for synthesis and workup, and the easily recoverable nature of that solvent. This emphasizes the importance of proper process design that must go beyond the synthetic step and needs to timely and holistically consider options for efficient downstream processing. Otherwise, efforts put into the optimization of an upstream synthesis may turn out futile if a technically, economically, or ecologically feasible downstream processing routine cannot be identified later.

The current *E* factor is already in a range comparable to the values expected for bulk chemicals, such as the envisaged biopolymers, in real industrial production facilities (1–5 kg kg<sup>-1</sup>).<sup>26</sup> For the specific production of styrene, however, the current commercial synthesis is petrochemical, involving high temperatures (500–600 °C) and harsh conditions, leading to significant waste production. In the search for more sustainable options, lignin-based approaches have been reported in the literature to enable the production of biobased monomers under milder conditions.<sup>18</sup> Moreover, other strategies involving metabolic engineering have proven successful, yet at rather low styrene titers, generating large volumes of wastewater in the process.<sup>18</sup> In the herein proposed system, the combination of process intensification, biocatalysis, and solvent recycling provides a promising low environmental impact. Importantly, since Green Chemistry calls for the minimization of waste generation, we reviewed the potential for further waste reductions in our process. Our first deliberation is based on

process intensification resulting in more and more favorable product-to-solvent ratios (Figure 4c). These in turn manifest themselves in substantial initial waste reductions and ultimately an asymptotic approach to a lower limit at high process intensities (dashed line). By extrapolation, the lowest *E* factor achievable by process intensification alone was estimated to be about 5.6 kg kg<sup>-1</sup>, as it ultimately removes the solvent waste component. This assumes otherwise constant stoichiometries and reuse rates. Improvements are also possible by means such as (i) more complete solvent recovery enabled by an integrated and automated reactor system (maximum reduction by ~1.4 kg kg<sup>-1</sup>); (ii) direct recovery and reuse of the sodium chloride solution used during workup (0.3 kg kg<sup>-1</sup>); (iii) in-house wastewater treatment facilitating water recycling (3.0 kg kg<sup>-1</sup>); or (iv) gas scrubbing of reactor exhaust gases to capture the released CO<sub>2</sub> to potentially recycle it as Na<sub>2</sub>CO<sub>3</sub> catalyst or quenching agent (0.6 kg kg<sup>-1</sup>).

Another important consideration regarding the environmental assessment is the total CO<sub>2</sub> formed during the synthesis of 1 kg product (expressed as kilograms of CO<sub>2</sub> generated per kg product). In the intended chemoenzymatic process, CO<sub>2</sub> is produced from several steps and sources. First, CO<sub>2</sub> generation occurs during the decarboxylation and quenching steps, which is considered to be neutral due to the biogenic origin of the substrates. Likewise, the process requires electrical energy and a biocatalyst, the generation of both contributes to the CO<sub>2</sub> footprint. Finally, two main waste streams will be generated: the organic fraction and the wastewater. The treatment of these streams will produce CO<sub>2</sub>, either during incineration (organic fraction) or during wastewater treatment (aqueous effluent). Ultimately, the combined assessment provides the total environmental impact of the reaction, measured as the total CO<sub>2</sub> release (TCR).

To get insights on this, the 10 L reaction producing 1.06 kg crude AMS served as a model. Energy inputs were estimated based on thermodynamic data and masses of the chemicals used (see Supporting Information), and accounted for the following steps: (a) heat the reaction from 20 to 30 °C and hold it for 4.5 h (enzymatic reaction); (b) heat the reaction system from 30 to 85 °C and hold it for 2 h (chemical reaction); (c) cool down from 85 to 60 °C and hold it for 1 h (quenching step); (d) cool down from 60 to 33 °C; (e) distill the CPME to recover the solvent and to obtain the crude product. All steps were assumed to follow an ideal behavior, and 25% excess energy was incorporated into the computation to account for inefficiencies, energy losses, etc. To estimate the CO<sub>2</sub> footprint associated with these energy needs, we presumed that all processes are powered with electricity from the average European Union energy mix, which as of 2022 corresponded to 251 g CO<sub>2</sub> per kWh.<sup>35</sup> Likewise, two main waste effluents were obtained: on the one hand, a total of 10.7 L CPME were used, of which 84% were recovered in reusable quality in the final distillation step. We expect it to be possible to reuse the recovered solvent for a minimum of 3 cycles, which results in a net use of 4.4 L of CPME per 1 kg crude product. This aliquot solvent fraction is then assumed to be incinerated, and the amount of CO<sub>2</sub> generated was calculated according to the stoichiometric CO<sub>2</sub> release: 1 mol CPME → 6 mol CO<sub>2</sub>.<sup>29,30</sup> On the other hand, 3.04 L of contaminated water accumulated per kg crude product.

The overall wastewater effluent additionally contained NaCl (0.34 kg), Na<sub>2</sub>CO<sub>3</sub> (0.037 kg), Na<sub>2</sub>SO<sub>4</sub> (0.02 kg), sodium acetate (1.521 kg), and some organic residues. All main



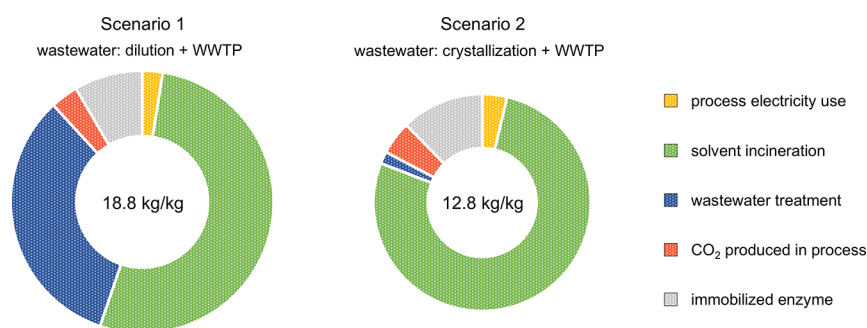


**Figure 5.** Estimated total CO<sub>2</sub> generation by the presented synthesis of AMS on a 10 L reactor scale, expressed in kg of CO<sub>2</sub> per kg of product. Multiple aspects were taken into account for the CO<sub>2</sub> production: (i) Yellow: Contribution by the electrical energy required to drive the process; (ii) Green: Contribution derived from the incineration of the organic waste fraction; (iii) Blue: Contribution from the wastewater treatment of the aqueous effluent, considering either 4-fold dilution (Scenario 1, left), or crystallization of sodium acetate (Scenario 2, right) prior the wastewater treatment plant (WWTP); (iv) Red: Estimated CO<sub>2</sub> released during the enzymatic decarboxylation and the reaction quench; and (v) Gray: CO<sub>2</sub> contribution from the immobilized enzyme preparation. See [Supporting Information](#) for details on calculations.

constituents are classified as “Water Hazard Class 1” (WGK 1), or “slightly hazardous to water”, according to the Rigoletto database.<sup>36</sup> Therefore, at this point, it was considered that the effluent could be sent to a conventional wastewater treatment plant (WWTP) for mild treatment leading to low CO<sub>2</sub> production. It must be noted, though, that processes must be assessed experimentally, as sometimes impurities are generated that may interfere with conventional wastewater treatment methods.<sup>30</sup> Given that sodium acetate comprises a sizable portion of the wastewater (31 wt %), two scenarios were investigated: (i) 4-fold dilution of the wastewater effluent before the WWTP, to ensure concentrations below the threshold for wastewater treatment microorganisms, and (ii) crystallization of sodium acetate before the WWTP to recover a valuable chemical before waste treatment. In either case, CO<sub>2</sub> production was estimated from total carbon dioxide release (TCR) values for mild wastewater treatment.<sup>30</sup> Details of the overall CO<sub>2</sub> production are depicted in [Figure 5](#).

Depending on the wastewater treatment strategy, we gauge the total CO<sub>2</sub> production at either ~19 kg (scenario 1: dilution/WWTP) or ~13 kg (scenario 2: crystallization/WWTP) carbon dioxide per kg product. This is consistent with data reported in the literature on industrial biotransformations at similar substrate concentrations of 100 g/L.<sup>28</sup> The largest contribution is attributed to solvent incineration or mineralization (~10 kg CO<sub>2</sub>), even when most of the solvent was recovered and reused for 3 cycles. Further measures to reduce solvent use (even greater process intensification, extended recycling) are clear options for further improvements. Similarly, the implementation of a crystallization step in the wastewater treatment may allow for the removal of a large part of the total dissolved carbon from the aqueous effluent (sodium acetate) and thus poses an interesting option to significantly reduce the environmental footprint compared to a simple dilution and wastewater treatment. Moreover, the isolation and potential marketing of sodium acetate may provide important commercial incentives for the overall process. Furthermore, as shown in [Figure 5](#) (gray section), the contributions from enzyme production and immobilization are also relevant to the overall CO<sub>2</sub> production. Thus, improved reusability of the biocatalyst is very much desirable from both an economic and environmental perspective. With respect to the carbon footprint arising from the generation of the electrical energy necessary for the process, the use of renewable energy for the electrical supply may also improve

the TCR of the process, assuming, for instance, hydropower energy with a production of 40 g CO<sub>2</sub> per kWh (~6 times less than the average EU energy mix in 2022).<sup>37</sup> An important lesson herein is the need for more research on and use of renewable energy in chemical plants. Finally, some CO<sub>2</sub> is produced from the substrate decarboxylation and reaction quenching steps, although that contribution is assumed to be biogenic and therefore neutral from an environmental perspective. In that respect, the incorporation of biogenic CPME – or other biogenic solvents – may effectively alleviate much of the remaining environmental burden. Overall, the intensified and scaled process shows promising sustainability metrics, and can certainly be further improved by taking actions on the highlighted hotspots of, e.g., solvent and enzyme use.

## CONCLUSIONS

A current frontier in biocatalytic research is the use of enzymes as efficient catalysts to produce high-volume low-value biobased chemicals, such as the herein reported styrene monomers. Their current large petrochemical production and versatile applications make them an important target to address. As the economics of the overall synthetic pipeline are tight, intensified processes that can make proper (re)use of employed resources are desired. Moreover, the genetic design of (more) robust enzymes with competitive turnovers at lower catalyst loadings, together with better recyclability can create more economically attractive options for bulk chemistry applications. With that in mind, the proposed synthetic route represents an important step in this direction and is enabled by the following key characteristics: (i) combination of bio- and chemocatalyst in the same organic solvent, simplifying the overall process and decreasing its environmental footprint; (ii) setup of an intensified process leading to high substrate loadings and yields (>100 g L<sup>-1</sup>; >95%); (iii) feasibility to recycle the solvent and the enzymes, reducing costs and associated wastes; (iv) promising environmental metrics of the kilogram-scaled system, based on the *E* factor and the total CO<sub>2</sub> released. Importantly, the current routine still offers potential for further improvements, such as its solvent use—for which better recycling can be envisaged on industrial fully automatized devices—and the design of an even more robust and reusable biocatalyst. Likewise, the future implementation of renewable energy together with adequate industrial heat integration, may contribute to decreasing the environmental

impact from the used energy. In trying to transcend the specific chemistry of this work, we accentuate the utility of integrating adequate environmental assessment into the early stages of chemical process development, as it provides valuable insights and guides the purposeful design of future intensified and sustainable processes for the chemical industry.

## MATERIALS AND METHODS

**General Information.**  $^1\text{H}$ - and  $^{13}\text{C}$  NMR spectra were recorded on a 400 MHz instrument (BRUKER) at +25 °C. Chemical shifts are given in parts per million (ppm) relative to solvent residual peaks of  $\text{CDCl}_3$  ( $^1\text{H}$ :  $\delta = 7.26$  ppm,  $^{13}\text{C}$ :  $\delta = 77.2$  ppm) and coupling constants ( $J$ ) are reported in Hertz (Hz). The phenolic acid decarboxylase used in this study (origin: *Bacillus subtilis*, PDB: 2P8G)<sup>23</sup> was heterologously expressed in *E. coli*, immobilized on ECR8415F, and immobilization yield, activity yield, as well as specific activity assessed as reported in previous works.<sup>20,21</sup> All synthetic procedures are provided in the Supporting Information.

**Materials.** All chemicals, materials, and solvents were obtained from commercial suppliers (Sigma-Aldrich, TCI Chemicals, VWR International, Merck KGaA, Thermo Fisher Scientific, ARMAR AG, Biowest, Air Liquide Gas AB, Purolite Ltd.) and used as received: ferulic acid (FA,  $\geq 99\%$  grade), *p*-coumaric acid (*p*CA,  $> 98.0\%$ ), sodium carbonate ( $\text{Na}_2\text{CO}_3$ ,  $\geq 97\%$ , technical), sodium chloride ( $\text{NaCl}$ , 100.0%, ACS grade), sodium sulfate ( $\text{Na}_2\text{SO}_4$ , anhydrous,  $\geq 99.0\%$ , p.a.), dipotassium hydrogen phosphate ( $\text{K}_2\text{HPO}_4$ , 99%), potassium dihydrogen phosphate ( $\text{KH}_2\text{PO}_4$ ,  $\geq 99.5\%$ ), acetic anhydride ( $\text{Ac}_2\text{O}$ , for synthesis), glutaraldehyde (50 wt % in water), cyclopentyl methyl ether (CPME, EMPLURA, 100%,  $> 10$  ppm BHT), acetonitrile (MeCN,  $\geq 99.8\%$ , HPLC grade), formic acid (99–100%), chloroform-*d* ( $\text{CDCl}_3$ , 99.8 atom % D, stab. with Ag), Bradford assay solution (Art. No. B5702), bovine serum albumin (BSA, lyophilized), deionized water (Milli-Q grade, 18.2 M $\Omega$  cm), and amino-functionalized Lifetech ECR8415F (Purolite Ltd.) for enzyme immobilization.

**Reaction Sampling and Analysis.** The reaction progress of all preparative syntheses was monitored by periodic sampling of either reaction step. Samples were taken using either piston stroke pipettes (0.12 L reactions) or a well-flushed sampling line with syringe (10 L reaction) and diluted in water/acetonitrile (1/1 v/v), vortexed, centrifuged (13,200 rpm, 2 min), and subjected to HPLC analysis. Particularly swift sampling and dilution was necessary during the acetylation step, as the otherwise cooling reaction mixture would congeal due to rapid product precipitation. To avoid such problems at scale, tempered sampling lines are indicated.

**High-Performance Liquid Chromatography.** Quantitative analyses were performed with a Shimadzu HPLC system (dwell volume determined to 0.33 mL) consisting of a SCL-10Avp system controller, a DGU-14A degasser, two LC-10ADvp pumps, a SIL-10ADvp autoinjector, a CTO-10ASvp column oven, and an SPD-M10Avp detector, all controlled by LabSolutions software (Shimadzu). The sample injection volume was 10  $\mu\text{L}$ , the column oven temperature  $35 \pm 0.5$  °C, the total flow rate 0.7 mL  $\text{min}^{-1}$ . Water and acetonitrile (MeCN) mixed with 0.1 vol % formic acid were used as eluents in an isocratic method: 0–10 min (55% MeCN) on Kinetex 5  $\mu\text{m}$  C18 100 Å, 250  $\times$  4.6 mm column (Phenomenex, 00G-4601-E0) protected by a SecurityGuard ULTRA C18 guard column. The 300 nm channel of the diode array detector was used for calibration and quantification of ferulic acid and *p*-coumaric acid. For conversion control using product-to-intermediate ratios in the chemical acetylation, the 254 nm channel was used. Calibrations are provided in the Supporting Information.

## ASSOCIATED CONTENT

### Data Availability Statement

The data underlying this study are openly available in Zenodo at <https://zenodo.org/records/13235085>.

## Supporting Information

The Supporting Information is available free of charge at <https://pubs.acs.org/doi/10.1021/acssuschemeng.4c03648>.

BsPAD dry solvent resiliency, procedures of lab and technical scale synthesis, annotated image of the 10 L rotating bed reactor, HPLC analytics, *E* factor system boundaries, *E* factor calculation, solvent reusability, catalyst reusability, and total carbon released (TCR) calculation (PDF)

## AUTHOR INFORMATION

### Corresponding Author

Selin Kara – Department of Biological and Chemical Engineering, Aarhus University, 8000 Aarhus C, Denmark; Institute of Technical Chemistry, Leibniz University Hannover, 30167 Hannover, Germany; [orcid.org/0000-0001-6754-2814](https://orcid.org/0000-0001-6754-2814); Email: [selin.kara@bce.au.dk](mailto:selin.kara@bce.au.dk)

### Authors

Philipp Petermeier – Department of Biological and Chemical Engineering, Aarhus University, 8000 Aarhus C, Denmark; SpinChem AB, 90736 Umeå, Sweden; [orcid.org/0000-0002-5007-9808](https://orcid.org/0000-0002-5007-9808)

Pablo Domínguez de María – Sustainable Momentum SL, 35011 Las Palmas de Gran Canaria, Canary Islands, Spain  
Emil Byström – SpinChem AB, 90736 Umeå, Sweden

Complete contact information is available at:

<https://pubs.acs.org/doi/10.1021/acssuschemeng.4c03648>

### Author Contributions

P.P. established the methodology, performed all experimental investigations and validations, conducted formal analysis and data visualization, and contributed to conceptualization. P.D.M. provided important formal analysis and contributed to the conceptualization and visualization of the research. E.B. provided resources for the project. S.K. acquired funding, and conceptualization, and provided resources. The manuscript was written through the contributions of all authors. All authors have given approval to the final version of the manuscript.

### Funding

This project has received funding from the European Union's Horizon 2020 research and innovation program under the Marie Skłodowska-Curie grant agreement no. 860414.

### Notes

The authors declare no competing financial interest.

## ACKNOWLEDGMENTS

The authors thank Prof. Robert Kourist from TU Graz (AT) for the kind provision of the BsPAD gene and Dr. Alessandra Basso and Dr. Simona Serban from Purolite Ltd. (UK) for the provision of Lifetech immobilization carrier. We also gratefully acknowledge Dr. Tobias Sparman from Umeå University (SE) for access to NMR analytics and Dr. Tobias Jonsson from Diduco AB (SE) for access to HPLC analytics. For their steadfast support in the customization and set up of the 10 L Complete S4 rotating bed reactor we thank Pierre Rönnqvist, Erik Löfgren, and Fritiof Pontén from SpinChem AB (SE) as well as Lars Eklund.



## ABBREVIATIONS

Ac<sub>2</sub>O, acetic anhydride; AMS, 4-acetoxy-3-methoxystyrene; AS, 4-acetoxystyrene; BHT, butylhydroxytoluene; BSA, bovine serum albumin; CPME, cyclopentyl methyl ether; ECR, enzyme carrier resin; FA, ferulic acid; GDP, gross domestic product; HPLC, high-performance liquid chromatography; MeCN, acetonitrile; NMR, nuclear magnetic resonance; pCA, p-coumaric acid; RBR, rotating bed reactor; 4VG, 4-vinylguaiacol; 4VP, 4-vinylphenol

## REFERENCES

- (1) Statistics Division, U. N., *Energy Balance Visualization. United Nations*, 2023: <https://unstats.un.org/unsd/energystats/dataPortal/> (accessed 2024-04-23).
- (2) *Plastics- the fast Facts 2023*; Plastics Europe, 2024: <https://plasticseurope.org/knowledge-hub/plastics-the-fast-facts-2023/> (accessed 2024-04-23).
- (3) Hirai, T.; Kawada, J.; Narita, M.; Ikawa, T.; Takeshima, H.; Satoh, K.; Kamigaito, M. Fully bio-based polymer blend of polyamide 11 and Poly(vinylcatechol) showing thermodynamic miscibility and excellent engineering properties. *Polymer* **2019**, *181*, No. 121667.
- (4) Sha, X.-L.; Yuan, L.; Liang, G.; Gu, A. Development and Mechanism of High-Performance Fully Biobased Shape Memory Benzoxazine Resins with a Green Strategy. *ACS Sustainable Chem. Eng.* **2020**, *8* (50), 18696–18705.
- (5) Messerschmidt, M.; Millaruelo, M.; Komber, H.; Häussler, L.; Voit, B.; Krause, T.; Yin, M.; Habicher, W.-D. Synthesis of Partially Protected Block Copolymers Based on 4-Hydroxystyrene Using NMRP and a Sequence of Polymer Analogous Reactions. *Macromolecules* **2008**, *41* (8), 2821–2831.
- (6) Degawa, K.; Matsumoto, A. Retardation Effect of Catechol Moiety during Radical Copolymerization of 3,4-Dihydroxystyrene with Various Monomers. *Chem. Lett.* **2019**, *48* (8), 928–931.
- (7) Takeshima, H.; Satoh, K.; Kamigaito, M. Bio-Based Functional Styrene Monomers Derived from Naturally Occurring Ferulic Acid for Poly(vinylcatechol) and Poly(vinylguaiacol) via Controlled Radical Polymerization. *Macromolecules* **2017**, *50* (11), 4206–4216.
- (8) van Schijndel, J.; Molendijk, D.; van Beurden, K.; Canalle, L. A.; Noël, T.; Meuldijk, J. Preparation of bio-based styrene alternatives and their free radical polymerization. *Eur. Polym. J.* **2020**, *125*, No. 109534.
- (9) Takeshima, H.; Satoh, K.; Kamigaito, M. Scalable Synthesis of Bio-Based Functional Styrene: Protected Vinyl Catechol from Caffeic Acid and Controlled Radical and Anionic Polymerizations Thereof. *ACS Sustainable Chem. Eng.* **2018**, *6* (11), 13681–13686.
- (10) Qian, Z.; Lou, Y.; Li, Q.; Wang, L.; Fu, F.; Liu, X. Novel Combination of Vinyl Benzoxazine and Its Copolymerizable Diluent with Outstanding Processability for Preparing a Bio-Based Thermoset. *ACS Sustainable Chem. Eng.* **2021**, *9* (32), 10929–10938.
- (11) Takeshima, H.; Satoh, K.; Kamigaito, M. Bio-based vinylphenol family: Synthesis via decarboxylation of naturally occurring cinnamic acids and living radical polymerization for functionalized polystyrenes. *J. Polym. Sci.* **2020**, *58* (1), 91–100.
- (12) Isikgor, F. H.; Becer, C. R. Lignocellulosic biomass: a sustainable platform for the production of bio-based chemicals and polymers. *Polym. Chem.* **2015**, *6* (25), 4497–4559.
- (13) Timokhin, V. I.; Regner, M.; Motagamwala, A. H.; Sener, C.; Karlen, S. D.; Dumesic, J. A.; Ralph, J. Production of p-Coumaric Acid from Corn GVL-Lignin. *ACS Sustainable Chem. Eng.* **2020**, *8* (47), 17427–17438.
- (14) Thi Truong, H.; Do Van, M.; Duc Huynh, L.; Thi Nguyen, L.; Do Tuan, A.; Le Xuan Thanh, T.; Duong Phuoc, H.; Takenaka, N.; Imamura, K.; Maeda, Y. A Method for Ferulic Acid Production from Rice Bran Oil Soapstock Using a Homogenous System. *Appl. Sci.* **2017**, *7* (8), 796.
- (15) Na, Y.; Chen, C. Catechol-Functionalized Polyolefins. *Angew. Chem., Int. Ed. Engl.* **2020**, *59* (20), 7953–7959.
- (16) Leibig, D.; Müller, A. H. E.; Frey, H. Anionic Polymerization of Vinylcatechol Derivatives: Reversal of the Monomer Gradient Directed by the Position of the Catechol Moiety in the Copolymerization with Styrene. *Macromolecules* **2016**, *49* (13), 4792–4801.
- (17) Zhang, W.; Wang, R.; Sun, Z.; Zhu, X.; Zhao, Q.; Zhang, T.; Cholewinski, A.; Yang, F. K.; Zhao, B.; Pinnaratip, R.; Forooshani, P. K.; Lee, B. P. Catechol-functionalized hydrogels: biomimetic design, adhesion mechanism, and biomedical applications. *Chem. Soc. Rev.* **2020**, *49* (2), 433–464.
- (18) Hayes, G.; Laurel, M.; MacKinnon, D.; Zhao, T.; Houck, H. A.; Becer, C. R. Polymers without Petrochemicals: Sustainable Routes to Conventional Monomers. *Chem. Rev.* **2023**, *123* (5), 2609–2734.
- (19) Avasthi, K.; Bohre, A.; Grilc, M.; Likozar, B.; Saha, B. Advances in catalytic production processes of biomass-derived vinyl monomers. *Catal. Sci. Technol.* **2020**, *10* (16), 5411–5437.
- (20) Petermeier, P.; Bittner, J. P.; Müller, S.; Byström, E.; Kara, S. Design of a green chemoenzymatic cascade for scalable synthesis of bio-based styrene alternatives. *Green Chem.* **2022**, *24* (18), 6889–6899.
- (21) Petermeier, P.; Bittner, J. P.; Jonsson, T.; Domínguez de María, P.; Byström, E.; Kara, S. Integrated preservation of water activity as key to intensified chemoenzymatic synthesis of bio-based styrene derivatives. *Commun. Chem.* **2024**, *7*, 57.
- (22) de Gonzalo, G.; Alcántara, A. R.; Domínguez de María, P. Cyclopentyl Methyl Ether (CPME): A Versatile Eco-Friendly Solvent for Applications in Biotechnology and Biorefineries. *ChemSusChem* **2019**, *12* (10), 2083–2097.
- (23) Joint Center for Structural Genomics, *Crystal structure of phenolic acid decarboxylase (2635953) from Bacillus subtilis at 1.36 Å resolution. RCSB Protein Data Bank*, 2007: <https://www.rcsb.org/structure/2P8G>.
- (24) Domínguez de María, P. Biocatalysis, sustainability, and industrial applications: Show me the metrics. *Curr. Opin. Green Sustainable Chem.* **2021**, *31*, No. 100514.
- (25) Vernet, G.; Hobisch, M.; Kara, S. Process intensification in oxidative biocatalysis. *Curr. Opin. Green Sustain. Chem.* **2022**, *38*, No. 100692.
- (26) Sheldon, R. A. The E factor at 30: a passion for pollution prevention. *Green Chem.* **2023**, *25* (5), 1704–1728.
- (27) Sheldon, R. A. Green chemistry and biocatalysis: Engineering a sustainable future. *Catal. Today* **2024**, *431*, No. 114571.
- (28) Domínguez de María, P.; Kara, S.; Gallou, F. Biocatalysis in Water or in Non-Conventional Media? Adding the CO<sub>2</sub> Production for the Debate. *Molecules* **2023**, *28* (18), 6452.
- (29) Onken, U.; Koettgen, A.; Scheidat, H.; Schuepp, P.; Gallou, F. Environmental Metrics to Drive a Cultural Change: Our Green Eco-Label. *Chimia (Aarau)* **2019**, *73* (9), 730–736.
- (30) Krell, C.; Schreiber, R.; Hueber, L.; Sciascera, L.; Zheng, X.; Clarke, A.; Haenggi, R.; Parmentier, M.; Baguia, H.; Rodde, S.; Gallou, F. Strategies to Tackle the Waste Water from  $\alpha$ -Tocopherol-Derived Surfactant Chemistry. *Org. Process Res. Dev.* **2021**, *25* (4), 900–915.
- (31) Domínguez de María, P.; Kara, S. On the fate of deep eutectic solvents after their use as reaction media: the CO<sub>2</sub> production during downstream and ultimate disposal. *RSC Sustainability* **2024**, *2* (3), 608–615.
- (32) Mallin, H.; Muschiol, J.; Byström, E.; Bornscheuer, U. T. Efficient Biocatalysis with Immobilized Enzymes or Encapsulated Whole Cell Microorganism by Using the SpinChem Reactor System. *ChemCatChem.* **2013**, *5* (12), 3529–3532.
- (33) Domínguez de María, P. On the need for gate-to-gate environmental metrics in biocatalysis: fatty acid hydration catalyzed by oleate hydratases as a case study. *Green Chem.* **2022**, *24* (24), 9620–9628.
- (34) Fadlallah, S.; Sinha Roy, P.; Garnier, G.; Saito, K.; Allais, F. Are lignin-derived monomers and polymers truly sustainable? An in-depth green metrics calculations approach. *Green Chem.* **2021**, *23* (4), 1495–1535.

(35) EEA, Greenhouse gas emission intensity of electricity generation. In *Data and maps*, 2024, [https://www.eea.europa.eu/data-and-maps/daviz/co2-emission-intensity-14#tab-chart\\_7](https://www.eea.europa.eu/data-and-maps/daviz/co2-emission-intensity-14#tab-chart_7), accessed 11.04.2024.

(36) Umweltbundesamt, Rigoletto, 2024. <https://webrigoletto.uba.de/Rigoletto/>, (accessed 12.04.2024).

(37) Delgove, M. A. F.; Laurent, A. B.; Woodley, J. M.; De Wildeman, S. M. A.; Bernaerts, K. V.; van der Meer, Y. A Prospective Life Cycle Assessment (LCA) of Monomer Synthesis: Comparison of Biocatalytic and Oxidative Chemistry. *ChemSusChem* **2019**, *12* (7), 1349–1360.